The Journal of Antibiotics (2015), 1–8

www.nature.com/ja

ORIGINAL ARTICLE

Graphiumins, new thiodiketopiperazines from the marine-derived fungus *Graphium* sp. OPMF00224

Takashi Fukuda[1], Minori Shinkai[1], Eri Sasaki[1], Kenichiro Nagai[1], Yuko Kurihara[2], Akihiko Kanamoto[2] and Hiroshi Tomoda[1]

Eight new thiodiketopiperazines, designated as graphiumins A to H (1–8), were isolated along with bisdethiobis(methylthio)-deacetylaranotin (9) and bisdethiobis(methylthio)-deacetylapoaranotin (10) from the culture broth of the marine-derived fungus *Graphium* sp. OPMF00224. The structures of the graphiumins were elucidated based on spectroscopic analyses (1D and 2D NMR data, ROESY correlations and CD data) and chemical methods. The absolute configuration of the common (3*S*)-3-hydroxy-octanoyl acid residue in 1, 3 and 4 was determined by hydrolysis, benzoyl derivatization and HPLC analysis using a chiral column. Five graphiumins moderately inhibited yellow pigment production by methicillin-resistant *Staphylococcus aureus*.
The Journal of Antibiotics advance online publication, 22 April 2015; doi:10.1038/ja.2015.41

INTRODUCTION

Methicillin-resistant *Staphylococcus aureus* (MRSA) is a major nosocomial pathogen that is resistant to many other antibiotics including currently used β-lactams.[1] Although vancomycin is widely used to treat MRSA infections, vancomycin-resistant *S. aureus* has been identified and reported.[2] Therefore, it has become increasingly important and necessary to discover new antibiotics effective against MRSA infections. *S. aureus* strains including MRSA produce a yellow pigment called staphyloxanthin.[3–5] Several research groups recently identified staphyloxanthin as one of the important virulence factors of *S. aureus*.[6–8] Staphyloxanthin is located in the cell membrane of *S. aureus* and has been associated with enhancing the survival and infectiousness of *S. aureus*.[5,6] Liu *et al.*[6] reported that the enzyme dehydrosqualene synthase-deficient mutant that could not produce staphyloxanthin failed to survive in a mouse host. This finding indicated that compounds inhibiting the production of staphyloxanthin could be a source of new anti-infectious agents against MRSA. On the basis of this concept, BPH-652,[7] zaragozic acid,[9] 7-benzyloxyindoles[10] and flavones[11] were reported to be inhibitors of staphyloxanthin production. We started to search for such inhibitors from natural sources using our established screening system,[12] leading to the discovery of tylopilusins[13] and citridone A and its derivatives.[14] Continuing our screening program, new compounds designated graphiumins A (**1**) to H (**8**), along with two structurally related known bisdethiobis(methylthio)-deacetylaranotin (**9**)[15] and bisdethiobis(methylthio)-deacetylapoaranotin (**10**),[15] were isolated from the culture broth of the marine-derived fungus *Graphium* sp. OPMF00224 (Figure 1). In this study, we describe the fermentation, isolation, structure elucidation and biological activity of these graphiumins.

RESULTS

Collection and identification of strain OPMF00224

Strain OPMF00224 was isolated from marine sediment collected at −17 m on Ishigaki Island, Okinawa, Japan. The sediment was treated by the direct inoculation method using kelp agar made with 130% artificial seawater (cut kelp 5 g, New Ocean (artificial sea water powder, Japan Bio Chemical) 46.8 g, agar 20 g, tap water 1l). The strain was cultured on Low Carbon Agar medium made with 100% artificial seawater for identification. DNA extraction, PCR, sequencing and Basic Local Alignment Search Tool searching followed.[16,17] The primer set ITS-5 (5′-GGAAGTAAAAGTCGTAACAAGG-3′) and NL-4 (5′-GGTCCGTGTTTCAAGACGG-3′) was used to amplify the region under the conditions of 30 cycles at 94 °C for 30 s, 60 °C for 30 s and 72 °C for 90 s. The sequence is available at the DNA Data Bank of Japan/European Molecular Biology Laboratory/GenBank databases under the accession number AB934385. On the basis of the Basic Local Alignment Search Tool search and its microscopic features, the strain was identified as a *Graphium* sp.

Fermentation

The strain was inoculated into a 500-ml Erlenmeyer flask containing 100 ml seed medium (2.0% glucose, 0.2% yeast extract, 0.05% $MgSO_4{\cdot}7H_2O$, 0.5% polypeptone, 0.1% KH_2PO_4 and 0.1% agar, pH 6.0). The flask was shaken on a rotary shaker at 27 °C for 3 days. The seed culture (2.0 ml) was transferred into a 1000-ml culture box containing 150 ml production medium (5.0% oat meal, 0.2% yeast extract, 0.1% Na tartrate, 0.1% KH_2PO_4, 0.8% DAIGO authentic seawater). Fermentation was carried out at 27 °C for 24 days under static conditions.

[1]Graduate School of Pharmaceutical Sciences, Kitasato University, Tokyo, Japan and [2]OP BIO FACTORY Co., Ltd, Okinawa, Japan
Correspondence: Professor H Tomoda, Graduate School of Pharmaceutical Sciences, Kitasato University, 5-9-1 Shirokane, Minato-ku, Tokyo 108-8641 Japan.
E-mail: tomodah@pharm.kitasato-u.ac.jp
Received 11 December 2014; revised 1 March 2015; accepted 24 March 2015

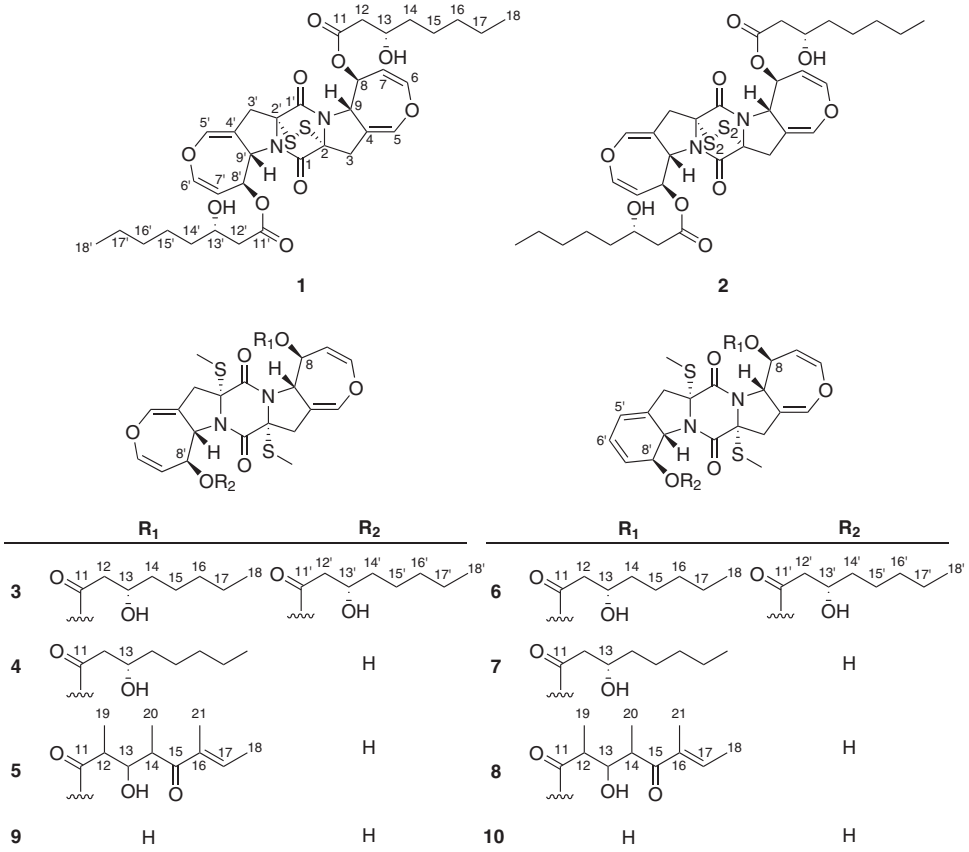

Figure 1 Structures of graphiumins A (**1**) to H (**8**), bisdethiobis(methylthio)-deacetylaranotin (**9**) and bisdethiobis(methylthio)-deacetylapoaranotin (**10**).

Isolation

The culture broth (150 ml × 30) was extracted with ethanol (4.5 l) for 2 h. After this extract had been evaporated to an aqueous solution, the residue was partitioned between water and ethyl acetate to yield the crude extract (600 mg) after the evaporation of the ethyl acetate fraction. The crude extract was dissolved in a small volume of chloroform, applied onto a silica gel column (30 g, 3.4 × 15 cm, 0.04–0.063 mm) and eluted stepwise with 100% chloroform, 50:1, 25:1, 10:1, 5:1, 1:1 (v/v) of chloroform-methanol solvent and 100% methanol (200 ml each). Graphiumins were observed in the last fraction eluted with 50:1 chloroform-methanol. This fraction was further purified by reversed-phase C-18 HPLC (10 × 250 mm; PEGASIL ODS, Senshu Scientific Co., Tokyo, Japan) under the following conditions: solvent, a 40-min linear gradient from 60 to 80% aqueous acetonitrile, at a flow rate of 3.0 ml min^{-1} with UV detection at 210 nm. Under this condition, graphiumins A, B, C, D, E, F, G, H, bisdethiobis(methylthio)-deacetylaranotin (**9**) and bisdethiobis (methylthio)-deacetylapoaranotin (**10**) were eluted as peaks with retention times of 30.0, 34.0, 31.4, 16.2, 12.3, 37.7, 18.5, 13.9, 7.6 and 8.5 min, respectively. These peaks were collected and concentrated to yield 1.0, 1.3, 4.2, 1.1, 17.1, 3.8, 3.5, 3.2, 2.5 and 1.7 mg as pale-yellow solids, respectively.

Physicochemical properties of graphiumins

The physicochemical properties of graphiumins are summarized in Table 1. All graphiumins showed very similar UV spectra with absorption maxima at 222 ~ 230 nm. Absorptions at 1730 ~ 1738 and 1656 ~ 1670 cm^{-1} in IR spectra suggested the presence of two kinds of carbonyl groups. These spectral similarities indicate that they are all structurally related.

Structure elucidation of graphiumins

Graphiumin A (**1**): graphiumin A (**1**) was obtained as a pale-yellow solid. The molecular formula for **1** was established as $C_{34}H_{44}N_2O_{10}S_2$ ($[M+Na]^+$ *m/z* 727.2343, calcd $[M+Na]^+$ 727.2335) on the basis of high-resolution ESI-MS measurements, indicating **1** contained 14 degrees of unsaturation (Table 1). ^1H and ^{13}C NMR data (in $CDCl_3$) supported the molecular formula (Tables 2 and 3). The ^{13}C NMR spectrum showed 17 resolved signals, which were classified into one methyl, six methylenes, six methines, including three sp^2 methines and four quaternary carbons, including two carbonyl carbons (C-1 and C-11). On the basis of its molecular formula, **1** appeared to be a symmetrical compound. The ^1H NMR spectrum of **1** showed one methyl signal, three olefinic methine signals, two oxygenated methine signals and many methylene signals. The connectivity of all proton and carbon atoms was established by HMQC experiments (Table 2). An analysis of ^1H-^1H COSY data allowed two partial structures I and II to be assigned (Figure 2). An analysis of HMBC spectroscopic data gave further structural information on **1**. The cross-peaks from H_2-3 (δ 2.98, 4.10) to C-1 (δ 162.5), C-2 (δ 79.7), C-4 (δ 112.9), C-5 (δ 139.6) and C-9 (δ 63.0) from H-5 (δ 6.62) to C-3, C-4 and C-6 (δ 141.4), from H-6 (δ 6.34) to C-5 and from H-9 (δ 5.11) to C-3 and C-4 supported the partial structure I. Additional cross-peaks from H-8 (δ 5.74) to C-11 (δ 171.5) and from H-12 (δ 2.46) to C-11 supported the connectivity of the partial structures I and II. The chemical shifts of C-1 and C-2 and the number of nitrogen and sulfur atoms present

Table 1 Physico-chemical properties of graphiumins A (1) to H (8)

	A (*1*)	*B* (*2*)	*C* (*3*)	*D* (*4*)	*E* (*5*)	*F* (*6*)	*G* (*7*)	*H* (*8*)
Appearance	*Pale-yellow solid*	*Pale-yellow solid*	*Pale-yellow solid*	*Pale-yellow solid*	*Pale-yellow solid*	*Pale-yellow solid*	*Pale-yellow solid*	*Pale-yellow solid*
$[\alpha]_D^{26}$ (*c* 0.1, MeOH)	−117°	−29°	−115°	−126°	−174°	−74°	−137°	−128°
Molecular formula	$C_{34}H_{44}N_2O_{10}S_2$	$C_{34}H_{44}N_2O_{10}S_4$	$C_{36}H_{50}N_2O_{10}S_2$	$C_{28}H_{36}N_2O_8S_2$	$C_{31}H_{38}N_2O_9S_2$	$C_{36}H_{50}N_2O_9S_2$	$C_{28}H_{36}N_2O_7S_2$	$C_{31}H_{38}N_2O_8S_2$
MW	704	768	734	592	646	718	576	630
HR ESI-MS *m/z*	$(M+Na)^+$	$(M+Na)^+$	$(M+Na)^+$	$(M+Na)^+$	$(M+Na)^+$	$(M+Na)^+$	$(M+Na)^+$	$(M+Na)^+$
Calcd	727.2335	797.1776	757.2804	615.1810	669.1916	741.2855	599.1861	653.1967
Found	727.2343	797.1769	757.2802	615.1807	669.1904	741.2845	599.1856	653.1964
$UV\lambda_{max}^{MeoH}$ nm (log ε)	227 (3.7)	223 (3.6)	225 (4.0)	227 (3.9)	230 (4.1)	227 (4.0)	222 (4.3)	227 (4.3)
$IR\gamma_{max}^{KBr}$ cm^{-1}	3458, 2956, 1731, 1656	3460, 2959, 1730, 1670	3498, 2957, 1736, 1670	3460, 2924, 1733, 1666	3462, 2924, 1730, 1657	3464, 2925, 1738, 1673	3429, 2924, 1733, 1672	3430, 2954, 1732, 1670
CD (MeOH)	224 (–40),	233 (–12),	225 (–11),	225 (–53),	224 (–47),	224 (–28),	224 (–39),	223 (–34),
λ nm (Mol. CD)	270 (0.1)	280 (0.63)	248 (–1.0)	248 (–3.0)	247 (–1.1)	257 (0.29)	255 (–1.6)	258 (0.03)
			254 (–1.3)	257 (–4.1)	258 (–3.2)	276 (3.4)	280 (3.7)	280 (3.0)

in **1** supported an aranotin type epidithiodiketopiperazine skeleton.[18] Taking its structural symmetry into consideration, the planar structure of **1** was elucidated.

The stereochemistry of the central ring part in **1** was determined by ROESY experiments, ^1H-^1H coupling constant measurements and CD data. The NOE correlations between 3-H and 5-H as well as between 8-H and 9-H and the coupling constants $J_{7\text{-}8}$ (2.0 Hz) and $J_{8\text{-}9}$ (8.5 Hz) indicated that **1** had the same configuration as known **9**. In addition, the CD spectrum of **1** exhibited a typical positive Cotton effect at 270 nm for a disulfide bridge on the diketopiperazine ring, indicating that **1** has the 2R/2′R configurations.[19] Accordingly, the stereochemistry of the central ring of **1** is as shown in Figure 2. Then, the absolute configuration of the hydroxylated carbon in the octanoyl side chain was determined by chiral HPLC analysis of the benzyl derivative of the base hydrolysate of **1**.[20] In the case of **1**, the peak was observed with a retention time of 29.8 min, indicating that the conformations of both C-13 and C-13′ were elucidated as *S* (Figure 3). On the basis of all data, the absolute structure of **1** was elucidated as shown in Figure 1.

Graphiumin B (**2**): the structure of **2** was elucidated by comparing all spectroscopic data with those of **1**. The molecular formula of **2** was established as $C_{34}H_{44}N_2O_{10}S_4$ ($[M+Na]^+$ *m/z* 797.1769, calcd $[M+Na]^+$ 797.1776) on the basis of high-resolution ESI-MS measurements, indicating that **2** was 64 mass units (S_2) larger than **1**. The similarity in the NMR spectra to **1** and its molecular formula indicated that it possessed at tetrasulphide in place of a disulfide bridge.

Graphiumin C (**3**): the molecular formula of **3** was established as $C_{36}H_{50}N_2O_{10}S_2$ ($[M+Na]^+$ *m/z* 757.2802, calcd $[M+Na]^+$ 757.2804) on the basis of high-resolution ESI-MS measurements, indicating that **3** was 30 mass units (C_2H_6) larger than **1** and contained 13 degrees of unsaturation (Table 1). The ^1H and ^{13}C NMR data (in $CDCl_3$) supported the molecular formula (Tables 2 and 3). The difference between **1** and **3** was that an additional methyl signal (C δ 14.8, H δ 2.28) in **3** was observed in the ^{13}C and ^1H NMR spectra (Tables 2 and 3). In addition, the cross-peak from S-CH_3 to C-2/2′ (δ 70.5) in **3** was observed in HMBC data (Figure 4). The CD spectrum of **3** exhibited a typical negative Cotton effect at 254 nm in two *S*-methyl groups on diketopiperazine ring, indicating that **3** has the 2R/2′R configurations.[19] All these data indicated that **3** was di-*S*-methylated **1**.

Graphiumin D (**4**): the molecular formula of **4** was established as $C_{28}H_{36}N_2O_8S_2$ ($[M+Na]^+$ *m/z* 615.1807, calcd $[M+Na]^+$ 615.1810) on the basis of high-resolution ESI-MS measurements, indicating that **4** was 142 mass units ($C_8H_{14}O_2$) smaller than **3**. The clear difference between **3** and **4** was that **4** was not a symmetrical compound. The ^{13}C NMR spectrum showed 28 resolved signals, which were classified into three methyls, seven methylenes, eleven methines including six sp^2 methines and seven quaternary carbons including three carbonyl carbons (C-1, C-11 and C-1′) (Table 2). An analysis of ^1H-^1H COSY data allowed three partial structures, C-6 to C-9, C-6′ to C-9′ and C-12 to C-18, to be assigned. In addition, the signals corresponding to one side chain in **4** were missing in the ^1H and ^{13}C NMR spectra. A broad signal assigned 8′-OH (δ 4.43) instead appeared in ^1H NMR. These data indicated that the structure of **4** was des-8′-*O* hydroxyoctanyl **3**. The structure satisfied the molecular formula and degrees of unsaturation.

Graphiumin E (**5**): the molecular formula of **5** was established as $C_{31}H_{38}N_2O_9S_2$ ($[M+Na]^+$ *m/z* 669.1904, calcd $[M+Na]^+$ 669.1916) on the basis of high-resolution ESI-MS measurements. The NMR spectra of **5** were similar to those of **4** (Tables 2 and 3). The clear difference between **4** and **5** lay in the side chain signals in the NMR data. The ^{13}C NMR spectrum showed 31 resolved signals, which were classified into six methyls, two methylenes, 14 methines including seven sp^2 methines

Table 2 ^{13}C NMR spectroscopic data for 1 to 8 in $CDCl_3$ (100 MHz for 1 and 3 and 150 MHz for 2, 4, 5, 6, 7 and 8)[a,b]

	1	*2*	*3*	*4*	*5*	*6*	*7*	*8*
Position	δ_C	δ_C	δ_C	δ_C	δ_C	δ_C	δ_C	δ_C
1	162.5, s	166.0, s	164.8, s	166.6, s	166.7, s	165.2, s	167.3, s	167.3, s
2	79.7, s	75.6, s	70.5, s	70.3, s	70.4, s	70.4, s	69.7, s	69.8, s
3	34.1, t	41.5, t	40.6, t	40.1, t	40.3, t	40.9, t	39.6, t	39.8, t
4	112.9, s	107.8, s	109.1, s	109.2, s	109.7, s	109.4, s	109.2, s	109.8, s
5	139.6, d	138.9, d	137.8, d	138.2, d	137.9, d	137.9, d	138.1, d	138.0, d
6	141.4, d	139.9, d	139.9, d	139.9, d	139.8, d	139.9, d	139.9, d	139.8, d
7	105.1, d	105.7, d	105.3, d	105.3, d	105.6, d	105.3, d	105.5, d	105.7, d
8	69.8, d	71.0, d	71.7, d	71.8, d	72.4, d	71.8, d	72.0, d	72.6, d
9	63.0, d	60.9, d	60.5, d	60.6, d	60.3, d	60.6, d	60.4, d	60.2, d
10								
11	171.5, s	172.0, s	171.6, s	171.5, s	174.6, s	171.5, s	171.4, s	174.6, s
12	42.0, t	42.5, t	42.1, t	42.2, t	42.6, d	42.1, t	42.2, t	42.6, d
13	67.5, d	67.7, d	67.4, d	67.4, d	72.2, d	67.6, d	67.4, d	72.3, d
14	36.5, t	36.8, t	36.6, t	36.6, t	41.1, d	37.4, t	36.6, t	41.2, d
15	25.3, t	25.2, t	25.2, t	25.2, t	205.8, s	25.3, t	25.2, t	206.0, s
16	31.7, t	31.7, t	31.7, t	31.7, t	137.4, s	31.8, t	31.7, t	137.9, s
17	22.6, t	22.6, t	22.6, t	22.6, t	138.5, d	22.5, t	22.6, t	138.6, d
18	14.0, q	14.1, q	14.0, q	14.0, q	15.1, q	14.0, q	14.0, q	15.1, q
19					12.2, q			12.4, q
20					13.6, q			13.5, q
21					11.0, q			11.1, q
1'	162.5, s	166.0, s	164.8, s	164.6, s	164.4, s	165.0, s	164.7, s	164.4, s
2'	79.7, s	75.6, s	70.5, s	69.4, s	69.3, s	74.1, s	73.3, s	73.2, s
3'	34.1, t	41.5, t	40.6, t	40.0, t	40.1, t	40.1, t	38.6, t	38.7, t
4'	112.9, s	107.8, s	109.1, s	107.7, s	107.7, s	133.4, s	131.4, s	131.5, s
5'	139.6, d	138.9, d	137.8, d	138.0, d	137.9, d	120.0, d	120.1, d	120.0, d
6'	141.4, d	139.9, d	139.9, d	137.7, d	137.6, d	125.3, d	122.9, d	122.9, d
7'	105.1, d	105.7, d	105.3, d	110.8, d	110.8, d	127.7, d	130.5, d	130.5, d
8'	69.8, d	71.0, d	71.7, d	72.6, d	72.6, d	75.6, d	74.3, d	74.3, d
9'	63.0, d	60.9, d	60.5, d	64.1, d	64.1, d	64.5, d	69.0, d	69.0, d
10'								
11'	171.5, s	172.0, s	171.6, s			171.8, s		
12'	42.0, t	42.5, t	42.1, t			43.0, t		
13'	67.5, d	67.7, d	67.4, d			67.4, d		
14'	36.5, t	36.8, t	36.6, t			37.5, t		
15'	25.3, t	25.2, t	25.2, t			25.2, t		
16'	31.7, t	31.7, t	31.7, t			31.8, t		
17'	22.6, t	22.6, t	22.6, t			22.5, t		
18'	14.0, q	14.1, q	14.0, q			14.0, q		
2-SMe			14.8, q	14.7, q	14.8, q	14.5, q	14.9, q	14.9, q
2'-SMe			14.8, q	14.9, q	14.8, q	14.8, q	14.7, q	14.8, q

[a]Assignments made by interpretation of HSQC and HMBC NMR data.
[b]Chemical shifts are shown with reference to $CDCl_3$ as δ 77.0.

and nine quaternary carbons including four carbonyl carbons (C-1, C-11, C-15 and C-1′) (Table 2). An analysis of ^1H-^1H COSY data allowed partial structure III to be assigned (Figure 4). An analysis of HMBC data gave further structural information on the side chain. The cross-peaks from H-12 (δ 2.55) to C-11 (δ 174.6), from H-13 (δ 4.09) to C-11, from H-14 (δ 3.37) to C-15 (δ 205.8), from H-17 (δ 6.78) to C-15, from H-18 (δ 1.88) to C-16 (δ 137.4) and C-17 (δ 138.5), from H-19 (δ 1.24) to C-11, C-12 (δ 42.6) and C-13 (δ 72.2), from H-20 (δ 1.20) to C-13, C-14 (δ 41.1) and C-15 and from H-21 (δ 1.75) to C-15, C-16 and C-17 supported partial structure III (Figure 4). In addition, the cross-peaks from H-8 (δ 5.72) to C-11 supported that partial structure III was linked to the central ring system at C-8. Taken together, the structure of **5** was elucidated as shown in Figure 1.

Graphiumin F (**6**): the molecular formula for **6** was established as $C_{36}H_{50}N_2O_9S_2$ ($[M+Na]^+$ *m/z* 741.2845, calcd $[M+Na]^+$ 741.2855) on the basis of high-resolution ESI-MS measurements indicating that **6** contained 13 degrees of unsaturation. The ^{13}C NMR spectrum showed 36 resolved signals, which were classified into four methyls, 12 methylenes, 12 methines including six sp^2 methines and eight quaternary carbons including two carbonyl carbons (C-1 and C-11) (Tables 2 and 3). The ^1H NMR spectrum of **6** showed four methyl signals, six olefinic methine signals, four oxygenated methine signals and many methylene signals. The NMR spectra of **6** were similar to those of **3** (Tables 2 and 3). The difference between **3** and **6** was that 5′-H (δ 5.96) and 6′-H (δ 5.97) in **6** were shifted to the upper field in the ^1H NMR spectrum. An analysis of ^1H-^1H COSY data allowed the

Table 3 ^{1}H NMR spectroscopic data for 1 to 8 in $CDCl_3$ (400 MHz for 1 and 3 and 600 MHz for 2, 4, 5, 6, 7 and 8)[a]

	1	*2*	*3*	*4*	*5*	*6*	*7*	*8*
Position	δ_H (*mult, J Hz*)[b]	δ_H (*mult, J Hz*)[b]	δ_H (*mult, J Hz*)[b]	δ_H (*mult, J Hz*)[b]	δ_H (*mult, J Hz*)[b]	δ_H (*mult, J Hz*)[b]	δ_H (*mult, J Hz*)[b]	δ_H (*mult, J Hz*)[b]
1								
2								
3	2.98, dt (19.0, 1.5), 4.10, dq (19.0, 1.0)	3.10, d (17.0), 3.36, dt (19.0, 2.0)	2.99, dt (19.0, 1.5), 3.03, dt (19.0, 1.0)	3.03, d (15.0), 3.09, d (15.0)	3.01, d (16.0), 3.10, d (16.0)	2.96, dt (16.0, 2.0), 3.04, d (16.0, 2.0)	3.03, d (15.0), 3.13, d (15.0)	3.05, d (16.0), 3.12, d (16.0)
4								
5	6.62, q (2.0)	6.58, br t (2.0)	6.58, br t (2.0)	6.60, t (2.5)	6.60, t (2.0)	6.55, bt (2.0)	6.60, t (2.5)	6.59, t (2.0)
6	6.34, dd (8.0, 2.0)	6.28, dd (8.0, 2.0)	6.32, dd (8.5, 2.5)	6.32, dd (7.5, 2.5)	6.31, dd (8.5, 2.0)	6.30, dd (8.5, 2.5)	6.31, dd (8.5, 2.5)	6.30, dd (7.5, 2.0)
7	4.56, dd (8.0, 2.0)	4.65, dd (8.0, 2.0)	4.66, dd (8.5, 2.0)	4.66, m	4.62, dd (8.0, 2.0)	4.64, dd (8.0, 2.0)	4.62, dd (8.5, 2.0)	4.62, dd (9.0, 2.0)
8	5.74, dt (8.5, 2.0)	5.30, m[c]	5.89, dt (8.0, 2.0)	5.91, dt (7.0, 2.0)	5.72, dt (7.0, 2.0)	5.88, dt (8.0, 2.0)	5.88, m	5.65, dt (8.0, 2.0)
9	5.11, dq (8.5, 2.0)	5.30, m[c]	5.17, dq (8.0, 2.0)	5.15, d (7.0)	5.21, br d (7.0)	5.15, d (8.0)	5.15, dd (8.0, 2.5)	5.20, dd (7.0, 1.5)
10								
11								
12	2.46, dd (17.0, 3.0)	2.56, dd (17.0, 9.0), 2.62, dd (17.0, 2.5)	2.45, dd (17.0, 9.0), 2.53, dd (17.0, 2.5)	2.45, dd (17.0, 10.0), 2.51, dd (17.0, 2.0)	2.55, m	2.43, dd (17.0, 9.0), 2.52, dd (17.0, 2.5)	2.43, dd (16.0, 10.0), 2.51, dd (16.0, 2.0)	2.54, m
13	4.00, m	4.08, m	4.04, m	4.05, m	4.09, t (6.5)	4.15, m	4.04, m	4.08, dd (7.0, 5.0)
14	1.45, m	1.46, m, 1.56, m	1.38, m, 1.51, m	1.38, m, 1.58, m	3.37 m	1.40, m, 1.52, m	1.37, m, 1.50, m	3.37 m
15	1.40, m	1.46, m, 1.62, m	1.42, m	1.34, m, 1.42, m		1.25-1.40, m[c]	1.30, m, 1.40, m	
16	1.25, m	1.25, m, 1.30, m	1.28, m	1.30, m		1.25-1.40, m[c]	1.26, m	
17	1.30, m	1.30, m	1.29, m	1.29, m	6.78, m	1.25-1.40, m[c]	1.28, m	6.76, m
18	0.88, t (8.0)	0.89, t (8.0)	0.88, t (8.0)	0.88, t (7.0)	1.88, dd (7.0, 1.0)	0.88, t[c]	0.87, t (7.0)	1.87, dd (7.0, 1.0)
19					1.24, d (7.0)			1.24, d (7.0)
20					1.20, d (7.0)			1.21, d (7.0)
21					1.75, t (1.0)			1.75, t (1.0)
1'								
2'								
3'	2.98, dt (19.0, 1.5), 4.10, dq (19.0, 1.0)	3.10, d (17.0), 3.36, dt (19.0, 2.0)	2.99, dt (19.0, 1.5), 3.03, dt (19.0, 1.0)	2.97, m	2.97, dt (19.0, 2.0), 3.01, dt (19.0, 2.0)	2.83, m, 3.04,m	2.90, d (16.0), 3.03, d (16.0)	2.90, dt (18.0, 1.5), 3.05, dt (18.0, 1.0)
4'								
5'	6.62, q (2.0)	6.58, br t (2.0)	6.58, br t (2.0)	6.55, br s	6.52, t (2.0)	5.96, m	5.92, m	5.93, m
6'	6.34, dd (8.0, 2.0)	6.28, dd (8.0, 2.0)	6.32, dd (8.5, 2.5)	6.20, dd (8.0, 2.5)	6.21, dd (8.0, 2.5)	5.97, m	5.88, m	5.87, m
7'	4.56, dd (8.0, 2.0)	4.65, dd (8.0, 2.0)	4.66, dd (8.5, 2.0)	4.90, dd (8.0, 2.0)	4.92, dd (8.0, 2.0)	5.54, d (9.0)	5.75, d (10.0)	5.75, br d (9.0)
8'	5.74, dt (8.0, 2.0)	5.30, m[c]	5.89, dt (8.0, 2.0)	4.65, m	4.68,dt (8.0, 1.0)	6.22, d (14.0)	4.91, d (12.0)	4.92, d (15.0)
9'	5.11, dq (9.0, 2.0)	5.30, m[c]	5.17, dq (8.0, 2.0)	4.86, bd (8.0)	4.87, bd (8.0)	5.21, d (14.0)	4.88, d (12.0)	4.88, d (15.0)
10'								
11'								
12'	2.46, dd (17.0, 3.0)	2.56, dd (17.0, 9.0), 2.62, dd (17.0, 2.5)	2.45, dd (17.0, 9.0), 2.53, dd (17.0, 2.5)			2.41, dd (17.0, 9.0), 2.59, dd (17.0, 2.5)		
13'	4.00, m	4.08, m	4.04, m			4.05, m		
14'	1.45, m	1.46, m, 1.56, m	1.38, m, 1.51, m			1.39, m, 1.50, m		
15'	1.40, m	1.46, m, 1.62, m	1.42, m			1.25-1.40, m[c]		
16'	1.25, m	1.25, m, 1.30, m	1.28, m			1.25-1.40, m[c]		
17'	1.30, m	1.30, m	1.29, m			1.25-1.40, m[c]		
18'	0.88, t (8.0)	0.89, t (8.0)	0.88, t (8.0)			0.88, t[c]		
2-SMe			2.28, s	2.29, s	2.28, s	2.25, s	2.28, s	2.28, s
2'-SMe			2.28, s	2.29, s	2.29, s	2.32, s	2.23, s	2.29, s
8'OH				4.43, brs	4.45, brs		5.37, brs	4.47, brs
13-OH	3.25, brs	ND	3.35, brs	3.38, brs	3.58, brs	3.57, brs	ND	3.58, brs
13'-OH	3.25, brs	ND	3.35, brs			3.28, brs		

Abbreviation: ND, not detected.
[a]Assignments made by interpretation of HSQC and HMBC NMR data.
[b]Chemical shifts are shown with reference to $CDCl_3$ as δ7.24.
[c]Overlapping.

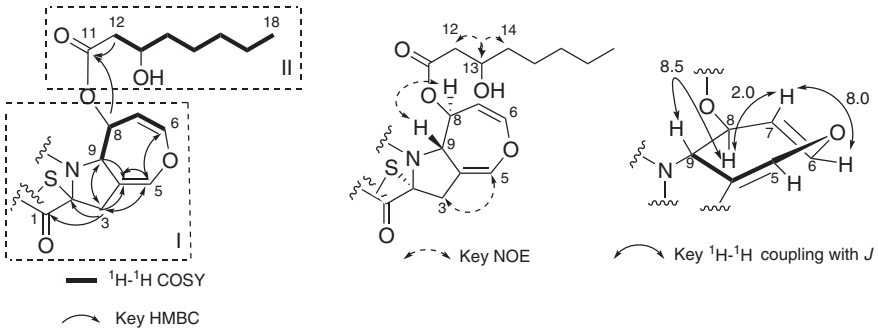

Figure 2 ^{1}H-^{1}H COSY, Key HMBC, NOE correlations and ^{1}H-^{1}H coupling of **1**.

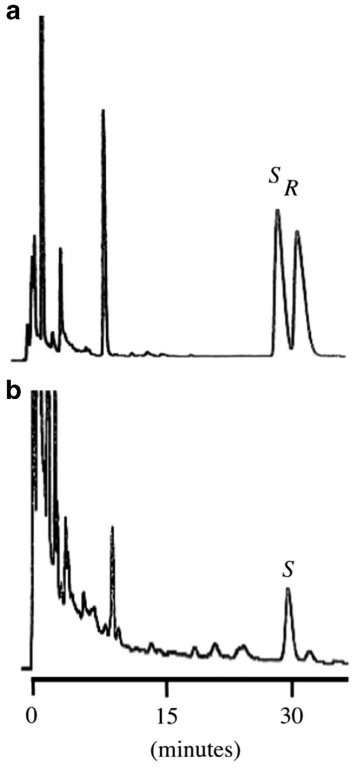

Figure 3 Separation of (*S*)benzyl-3-hydroxy-octanoate and (*R*)benzyl-3-hydroxy-octanoate by HPLC. (**a**) Derivatives prepared from authentic (±)-3-hydroxyoctanoic acid. (**b**) Derivative prepared from graphiumin A.

connectivity from C-5′ (δ 120.0) to C-9′ (δ 64.5) in the partial structure IV to be assigned (Figure 4). These results indicated that **6** was an apoaranotin type compound.[18] In addition, all data for the ring parts in **6** were similar to those of known bisdethiobis(methylthio)-deacetylapoaranotin (**10**).[15] The cross-peaks from 8-H (δ 5.88) to C-11 (δ 171.5) and from 8′-H (δ 6.22) to C-11′ (δ 171.8) in HMBC data supported the same acyl side chains was attached at both C-8 and C-8′. Taken together, the structure of **6** was elucidated as shown in Figure 1.

Graphiumin G (**7**): the molecular formula of **7** was established as $C_{28}H_{36}N_2O_7S_2$ ([M+Na]$^+$ *m/z* 599.1856, calcd [M+Na]$^+$ 599.1861) on the basis of high-resolution ESI-MS measurements, which was 142 mass units ($C_8H_{14}O_2$) smaller than **6**. This suggested that **7** was missing one side chain from **6**. In addition, the cross-peaks from H-8 (δ 5.88) to C-11 (δ 171.4) in HMBC supported that one acyl side chain was attached to C-8. Thus, the structure of **7** was elucidated as des-8′-*O* hydroxyoctanyl **6**.

Graphiumin H (**8**): the structure of **8** was elucidated by a comparison of all spectroscopic data with those of **5** and **6**. The molecular formula of **8** was established as $C_{31}H_{38}N_2O_8S_2$ ([M+Na]$^+$ *m/z* 653.1964, calcd [M+Na]$^+$ 653.1967) on the basis of high-resolution ESI-MS measurements, which was 16 mass units (O) smaller than **5**. In addition, **8** was an apoaranotin type from the chemical shifts of H-5′ (δ 5.93) and H-6′ (δ 5.87) with the same side chain as **5** (Tables 2 and 3). Taking all NMR data into consideration, the structure of **8** was elucidated as shown in Figure 1.

The absolute configurations of **3** and **4** were determined in the same way as **1**. In addition, taking the biogenetic mechanism, ROESY experiments and the value of optical rotation into consideration, **2**, **6**

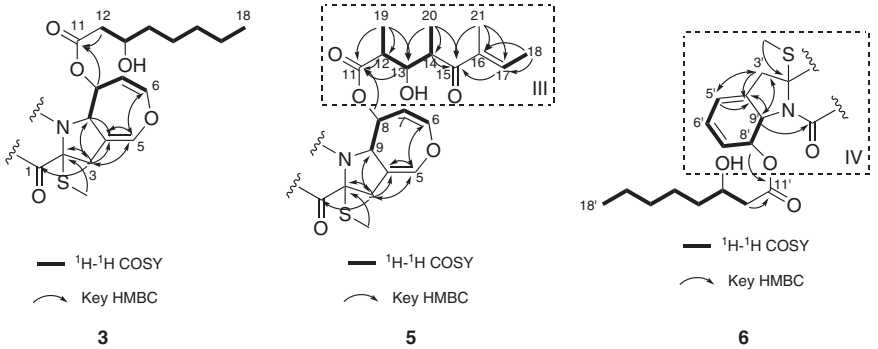

3 **5** **6**

Figure 4 ^{1}H-^{1}H COSY and Key HMBC correlations of **3**, **5** and **6**.

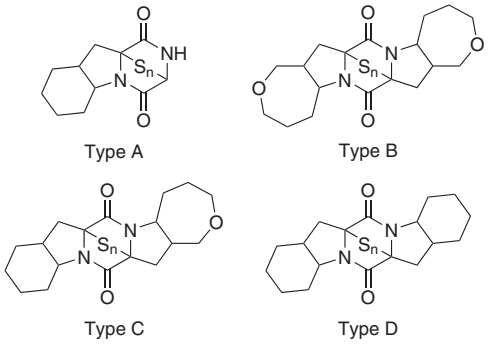

Figure 5 Structural classification of TDKPs.

and **7** were deduced to have the same absolute configurations. However, the absolute configurations for **5** and **8** are still unknown.

The effects of all graphiumins **1** to **10** on yellow pigment production by MRSA were tested using the paper disk method.[12] Compounds **1, 4, 5, 7, 8, 9, 10** and citridone A[14] (positive compound) showed a white zone (10, 14, 10, 12, 11, 11, 11 and 20 mm, respectively) with no inhibition zone at 50 μg 8 mm^{-1} paper disk, suggesting that they selectively inhibited the production of the yellow pigment without affecting the growth of MRSA.

DISCUSSION

A number of thiodiketopiperazines have been reported. On the basis of the core ring system consisting of carbon, oxygen and nitrogen atoms, they are classified into the four types as summarized in Figure 5. Type A has the three-ring system, to which gliotoxin[21] and phomazines A and B[22] belong. Type B has the symmetrical five-ring system including two oxepane rings, to which aranotin[17] and its derivatives[15] belong. Type C has the five-ring system including one oxepane ring, to which apoaranotin[17] and its derivatives[15] belong. Type D has the symmetrical five-ring system, to which a number of compounds such as epicoccins,[23] epicorazines,[24] rostratins,[25] haematocins,[26] scabrosin esters,[27] brocazines,[28] exserohilones,[29] phomazine C[22] and SCH64874s[30] belong. Graphiumins A (**1**) to E (**5**) belong to type B, and graphiumins F (**6**) to H (**8**) belong to type C. Regarding the side chain extending from the central ring, all of the eight graphiumins (**1** to **8**) have long acyl chains. Graphiumins E (**5**) and H (**8**) carry the same side chain of 3-hydroxy-2,4,6-trimethyl-5-oxooct-6-enoyl acid residue.[31,32] Before graphiumins discovery, only SCH64874s,[30] isolated from the culture broth of an unidentified fungus, had been reported to have two acyl side chains, whose planar structure is the same as that of **5** and **8**. Interestingly, the other graphiumins have the distinct 3-hydroxy-octanoyl acid residue(s) as the common side chain. Furthermore, **1**, **2**, **3** and **6** were found to be the second thiodiketopiperazines with the two acyl side chains. The biosynthesis of graphiumins remains to be investigated.

Structurally related thiodiketopiperazines were reported to possess various biological activities; aranotin with antiviral activity against polio and parainfluenza virus,[18,33] epicoccin A with antimicrobial activity,[23] epicoccin G with anti-HIV activity[34] and phomazines,[22] rostratins,[25] scabrosin esters[27] and brocazines[28] with cytotoxic activity. Accordingly, the graphiumins were evaluated in our in-house assays; antimicrobial assay,[35] mammalian cell cycle assay,[36] lipid metabolism assay[37] and bone morphogenetic protein-induced alkaline phosphatase expression assay.[38] However, they showed no activity in these assays even at 25 μg ml^{-1} (data not shown). Thus, compounds **1**, **4**, **5**, **7** and **8** selectively inhibited yellow pigment production by MRSA. The mechanism of action remains to be defined.

EXPERIMENTAL PROCEDURE

General experimental procedures

Optical rotations were recorded with a DIP-1000 digital polarimeter (JASCO, Tokyo, Japan). Melting points were measured with a micro melting apparatus (Yanaco, Kyoto, Japan). ESI-MS spectrometry was conducted on a JMS-T1000LP spectrometer (JEOL, Tokyo, Japan). UV and IR spectra were measured with a U-2800 spectrophotometer (HITACHI, Tokyo, Japan) and FT/IR-460 plus spectrometer (JASCO), respectively. The various NMR spectra were measured with an UNITY 400 or an INOVA 600 spectrometer (Agilent Technologies Inc, Santa Clara, CA, USA). Reversed-phase HPLC separations were performed using a Senshu pak preparative C18 PEGASIL ODS column (250 × 10 mm) at a flow rate of 3 ml min^{-1} and CHIRALCEL OJ-H column (150 × 4.6 mm) at a flow rate of 1.0 ml min^{-1} using the SHIMAZU LS20AT pump and SHIMAZU LS20AS UV detector.

Hydrolysis and benzoylation of graphiumins A, B and C

A total of 0.1N NaOH (1 ml) was added to a solution of a sample (0.5 mg) in a 1:3 mixture of water (250 μl) and methanol (750 μl) at room temperature. After stirring for 4 h, the resulting mixture was evaporated to give a colorless solid, which was used for the next reaction without further purification. Cesium carbonate (1 mg, 5 mmol) was added to a solution of the residue in water (100 μl) and the mixture was stirred at room temperature for 30 min. After removal of the solvent, the cesium salt was dissolved in dimethylformamide (100 μl) and benzyl bromide (10 μl) was then added. Stirring was continued at room temperature for 20 h. The resulting mixture was poured into a 1:1 mixture of water and ethyl acetate. The phases were separated and the aqueous phase was extracted with ethyl acetate. The combined organic phases were dried over Na_2SO_4, filtered and concentrated under reduced pressure. The residue was dissolved in MeOH (40 μl) for chiral HPLC analysis.

Analysis of stereochemistry of the benzyl-3-hydroxy-octanoate by HPLC

To determine the side chain stereochemistries, aliquots (20 μl) of the methanolic solutions of the benzyl derivatives of the base hydrolysates were analyzed using a SHIMAZU LS20AT pump under the following conditions: column, CHIRALCEL OJ-H column (150 × 4.6 mm); flow rate, 1.0 ml min^{-1}; detection, UV at 254 nm. Using 35% aqueous CH_3CN in 0.05% trifluoroacetic acid as a solvent for HPLC, benzyl (*3S*)-3-hydroxy-octanoate and benzyl (*3R*)-3-hydroxy-octanoate, which were synthesized from authentic (±)-3-hydroxyloctanoic acid (SIGMA-ALDRICH, St Louis, MO, USA) in the same manner, were eluted as peaks with retention times of 29.2 and 31.4 min, respectively (Figure 3). Under the same conditions, all products from graphiumins A, B and C were eluted as a peak with retention time of 29.2 min (Figure 3).

Assay for inhibition of yellow pigment production in MRSA using paper disks

MRSA K-24 strain, a clinical isolate, was used as a yellow pigment-producing strain. MRSA was cultured in Mueller–Hinton broth at 37 °C for 20 h and adjusted to 1 × 10^8 colony forming units/ml. The inoculum (100 μl) was spread on TYB agar (1.7% tryptone, 1% yeast extract, 0.5% NaCl, 0.25% K_2HPO_4, 15% agar and 1.5% monoacetate) (25 ml) on a plate (100 × 140 mm). Paper disks (8 mm i.d.) containing a 50 μg sample were placed on the plate and incubated at 37 °C for 72 h. Inhibition of the production of yellow pigments by a sample is expressed as the diameter (mm) of the white zone on the plate.

ACKNOWLEDGEMENTS

We wish to thank Ms Noriko Sato (School of Pharmaceutical Sciences, Kitasato University) for measuring the NMR spectra. This work was supported by Takeda Science Foundation (TF) and JSPS KAKENHI Grant Number 25870704 (TF).

1 Centers for Disease Control and Prevention (CDC). Staphylococcus aureus with reduced susceptibility to vancomycin–United States. *MMWR Morb. Mortal. Wkly. Rep.* **46**, 765–766 (1997).
2 Hiramatsu, K. *et al.* Methicillin-resistant *Staphylococcus aureus* clinical strain with reduced vancomycin susceptibility. *J. Antimicrob. Chemother.* **40**, 135–136 (1997).
3 Marshall, J. H. & Wilmoth, G. J. Pigments of *Staphylococcus aureus*, a series of triterpenoid carotenoids. *J. Bacteriol.* **147**, 900–913 (1981).
4 Marshall, J. H. & Wilmoth, G. J. Proposed pathway of triterpenoid carotenoid biosynthesis in *Staphylococcus aureus*: evidence from a study of mutants. *J. Bacteriol.* **147**, 914–919 (1981).
5 Clauditz, A., Resch, A., Wieland, K. P., Peschel, A. & Goötz, F. Staphyloxanthin plays a role in the fitness of *Staphylococcus aureus* and its ability to cope with oxidative stress. *Infect. Immun.* **74**, 4950–4953 (2006).
6 Liu, G. Y. *et al. Staphylococcus aureus* golden pigment impairs neutrophil killing and promotes virulence through its antioxidant activity. *J. Exp. Med.* **202**, 209–215 (2005)
7 Liu, C. I. *et al.* A cholesterol biosynthesis inhibitor blocks *Staphylococcus aureus* virulence. *Science* **319**, 1391–1394 (2008).
8 Song, Y. *et al.* Inhibition of staphyloxanthin virulence factor biosynthesis in *Staphylococcus aureus*: *in vitro*, *in vivo*, and crystallographic results. *J. Med. Chem.* **52**, 3869–3880 (2009).
9 Liu, C. I., Jeng, W. Y., Chang, W. J., Ko, T. P. & Wang, A. H. Binding modes of zaragozic acid A to human squalene synthase and staphylococcal dehydrosqualene synthase. *J. Biol. Chem.* **287**, 18750–18757 (2012).
10 Lee, J. H. *et al.* Indole and 7-benzyloxyindole attenuate the virulence of *Staphylococcus aureus*. *Appl. Microbiol. Biotechnol.* **97**, 4543–4552 (2013).
11 Lee, J. H., Park, J. H., Cho, M. H. & Lee, J. Flavone reduces the production of virulence factors, staphyloxanthin and α-hemolysin, in *Staphylococcus aureus*. *Curr. Microbiol.* **65**, 726–732 (2012).
12 Sakai, K. *et al.* Method of search for microbial inhibitors of staphyloxanthin production by MRSA. *Biol. Pharm. Bull.* **35**, 48–53 (2012).
13 Fukuda, T., Nagai, K. & Tomoda, H. (±)-Tylopilusins, diphenolic metabolites from the fruiting bodies of *Tylopilus eximius*. *J. Nat. Prod.* **75**, 2228–2231 (2012).
14 Fukuda, T., Shimoyama, T., Nagamitsu, T. & Tomoda, H. Synthesis and biological activity of citridone A and its derivatives. *J. Antibiot. (Tokyo)* **67**, 445–450 (2014).
15 Guo, C. J. *et al.* Biosynthetic pathway for the epipolythiodioxopiperazine acetylaration in *Aspergillus terreus* revealed by genome-based deletion analysis. *J. Am. Chem. Soc.* **135**, 7205–7213 (2013).
16 Kobayashi, K. *et al.* Bafilomycin L, a new inhibitor of cholesteryl ester synthesis in mammalian cells, produced by marine-derived Streptomyces sp. OPMA00072. *J. Antibiot. (Tokyo)* **68**, 126–132 (2015).
17 Kurihara, Y. *et al.* Entomopathogenic fungi isolated from suspended-soil-inhabiting arthropods in East Kalimantan, Indonesia. *Mycoscience* **49**, 241–249 (2008).
18 Neuss, N. *et al.* Aranotin and related metabolites from *Arachniotus aureus* (Eidam) Schroeter. IV. Fermentation, isolation, structure elucidation, biosynthesis, and antiviral properties. *Antimicrob. Agents Chemother.* **8**, 213–219 (1968).
19 Wang, J. M. *et al.* Study on absolute configurations of α/α' chiral carbons of thiodiketopiperazines by experimental and calculated circular dichroism spectra. *Tetrahedron* **69**, 1195–1201 (2013).
20 Nagai, K. *et al.* Synthesis and biological evaluation of a beauveriolide analogue library. *J. Comb. Chem.* **8**, 103–109 (2006).
21 Brian, P. W. & Hemming, H. G. Gliotoxin, a fungistatic metabolic product of *Trichoderma viride*. *Ann. Appl. Biol.* **32**, 214–220 (1945).
22 Kong, F., Wang, Y., Liu, P., Dong, T. & Zhu, W. Thiodiketopiperazines from the marine-derived fungus *Phoma* sp. OUCMDZ-1847. *J. Nat. Prod.* **77**, 132–137 (2014).
23 Wang, J. M. *et al.* Thiodiketopiperazines produced by the endophytic fungus *Epicoccum nigrum*. *J. Nat. Prod.* **73**, 1240–1249 (2010).
24 Deffieux, G., Baute, M. A., Baute, R. & Filleau, M. J. New antibiotics from the fungus *Epicoccum nigrum*. II. Epicorazine A: structure elucidation and absolute configuration. *J. Antibiot. (Tokyo)* **31**, 1102–1105 (1978).
25 Tan, R. X., Jensen, P. R., Williams, P. G. & Fenical, W. Isolation and structure assignments of rostratins A-D, cytotoxic disulfides produced by the marine-derived fungus *Exserohilum rostratum*. *J. Nat. Prod.* **67**, 1374–1382 (2004).
26 Suzuki, Y. *et al.* Haematocin, a new antifungal diketopiperazine produced by *Nectria haematococca* Berk. et Br. (880701a-1) causing nectria blight disease on ornamental plants. *J. Antibiot. (Tokyo)* **53**, 45–49 (2000).
27 Chai, C. L., Elix, J. A., Huleatt, P. B. & Waring, P. Scabrosin esters and derivatives: chemical derivatization studies and biological evaluation. *Bioorg. Med. Chem.* **12**, 5991–5995 (2004).
28 Meng, L. H., Li, X. M., Lv, C. T., Huang, C. G. & Wang, B. G. Brocazines A-F, cytotoxic bisthiodiketopiperazine derivatives from *Penicillium brocae* MA-231, an endophytic fungus derived from the marine mangrove plant *Avicennia marina*. *J. Nat. Prod.* **77**, 1921–1927 (2014).
29 Gross, U., Nieger, M. & Brase, S. A unified strategy targeting the thiodiketopiperazine mycotoxins exserohilone, gliotoxin, the epicoccins, the epicorazines, rostratin A and aranotin. *Chem. Eur. J* **16**, 11624–11631 (2010).
30 Hegde, V. R., Dai, P., Patel, M., Das, P. R. & Puar, M. S. Novel thiodiketopiperazine fungal metabolites as epidermal growth factor receptor antagonists. *Tet. Lett.* **38**, 911–914 (1997).
31 Chinworrungsee, M., Kittakoop, P., Saenboonrueng, J., Kongsaeree, P. & Thebtaranonth, Y. Bioactive compounds from the seed fungus *Menisporopsis theobromae* BCC 3975. *J. Nat. Prod.* **69**, 1404–1410 (2006).
32 Kawashima, A., Yoshimura, Y., Mizutani, T., Hanada, K. & Omura, S. Jpn. Kokai Tokkyo Koho Patent No. JP2062880 (19900302) (1990).
33 Trown, P. W. *et al.* LL-S88-alpha, an antiviral substance produced by *Aspergillus terreus*. *Antimicrob. Agents Chemother.* **8**, 225–228 (1968).
34 Zhang, Y., Liu, S. & Liu, X. Epicoccins A-D, epipolythiodioxopiperazines from a Cordyceps-colonizing isolate of *Epicoccum nigrum*. *J. Nat. Prod.* **70**, 1522–1525 (2007).
35 Iwatsuki, M. *et al.* Lariatins, novel anti-mycobacterial peptides with a lasso structure, produced by *Rhodococcus jostii* K01-B0171. *J. Antibiot.* **60**, 357–363 (2007).
36 Hagimori, K., Fukuda, T., Hasegawa, Y., Omura, S. & Tomoda, H. Fungal malformins inhibit bleomycin-induced G2 checkpoint in Jurkat cells. *Biol. Pharm. Bull.* **30**, 1379–1383 (2007).
37 Ohshiro, T. & Tomoda, H. Isoform-specific inhibitors of ACATs: recent advances and promising developments. *Future Med. Chem.* **3**, 2039–2061 (2011).
38 Fukuda, T. *et al.* Trichocyalides A and B, new inhibitors of alkaline phosphatase activity in bone morphogenetic protein-stimulated myoblasts, produced by *Trichoderma* sp. FKI-5513. *J. Antibiot. (Tokyo)* **65**, 565–569 (2012).